JCI The Journal of Clinical Investigation

β_{IV}-Spectrin regulates STAT3 targeting to tune cardiac response to pressure overload

Sathya D. Unudurthi, … , Peter J. Mohler, Thomas J. Hund

J Clin Invest. 2018;128(12):5561-5572. https://doi.org/10.1172/JCI99245.

Research Article **Cardiology**

Heart failure (HF) remains a major source of morbidity and mortality in the US. The multifunctional Ca^{2+}/calmodulin-dependent kinase II (CaMKII) has emerged as a critical regulator of cardiac hypertrophy and failure, although the mechanisms remain unclear. Previous studies have established that the cytoskeletal protein β_{IV}-spectrin coordinates local CaMKII signaling. Here, we sought to determine the role of a spectrin-CaMKII complex in maladaptive remodeling in HF. Chronic pressure overload (6 weeks of transaortic constriction [TAC]) induced a decrease in cardiac function in WT mice but not in animals expressing truncated β_{IV}-spectrin lacking spectrin-CaMKII interaction (*qv*^{3J} mice). Underlying the observed differences in function was an unexpected differential regulation of STAT3-related genes in *qv*^{3J} TAC hearts. In vitro experiments demonstrated that β_{IV}-spectrin serves as a target for CaMKII phosphorylation, which regulates its stability. Cardiac-specific β_{IV}-spectrin–KO (β_{IV}-cKO) mice showed STAT3 dysregulation, fibrosis, and decreased cardiac function at baseline, similar to what was observed with TAC in WT mice. STAT3 inhibition restored normal cardiac structure and function in β_{IV}-cKO and WT TAC hearts. Our studies identify a spectrin-based complex essential for regulation of the cardiac response to chronic pressure overload. We anticipate that strategies targeting the new spectrin-based "statosome" will be effective at suppressing maladaptive remodeling in response to chronic stress.

β_{IV}-Spectrin regulates STAT3 targeting to tune cardiac response to pressure overload

Sathya D. Unudurthi,[1,2] Drew Nassal,[1,2] Amara Greer-Short,[1,2] Nehal Patel,[1,2] Taylor Howard,[1,2] Xianyao Xu,[1] Birce Onal,[1,2] Tony Satroplus,[1,2] Deborah Hong,[1,2] Cemantha Lane,[1,2] Alyssa Dalic,[1,2] Sara N. Koenig,[1,3] Adam C. Lehnig,[1,3] Lisa A. Baer,[1,3] Hassan Musa,[1] Kristin I. Stanford,[1,3] Sakima Smith,[1,4] Peter J. Mohler,[1,3,4] and Thomas J. Hund[1,2,4]

[1]The Dorothy M. Davis Heart and Lung Research Institute, The Ohio State University Wexner Medical Center, Columbus, Ohio, USA. [2]Department of Biomedical Engineering, College of Engineering, The Ohio State University, Columbus, Ohio, USA. [3]Department of Physiology and Cell Biology, and [4]Department of Internal Medicine, The Ohio State University College of Medicine, Columbus, Ohio, USA.

Heart failure (HF) remains a major source of morbidity and mortality in the US. The multifunctional Ca^{2+}/calmodulin-dependent kinase II (CaMKII) has emerged as a critical regulator of cardiac hypertrophy and failure, although the mechanisms remain unclear. Previous studies have established that the cytoskeletal protein β_{IV}-spectrin coordinates local CaMKII signaling. Here, we sought to determine the role of a spectrin-CaMKII complex in maladaptive remodeling in HF. Chronic pressure overload (6 weeks of transaortic constriction [TAC]) induced a decrease in cardiac function in WT mice but not in animals expressing truncated β_{IV}-spectrin lacking spectrin-CaMKII interaction (qv^{3J} mice). Underlying the observed differences in function was an unexpected differential regulation of STAT3-related genes in qv^{3J} TAC hearts. In vitro experiments demonstrated that β_{IV}-spectrin serves as a target for CaMKII phosphorylation, which regulates its stability. Cardiac-specific β_{IV}-spectrin–KO (β_{IV}-cKO) mice showed STAT3 dysregulation, fibrosis, and decreased cardiac function at baseline, similar to what was observed with TAC in WT mice. STAT3 inhibition restored normal cardiac structure and function in β_{IV}-cKO and WT TAC hearts. Our studies identify a spectrin-based complex essential for regulation of the cardiac response to chronic pressure overload. We anticipate that strategies targeting the new spectrin-based "statosome" will be effective at suppressing maladaptive remodeling in response to chronic stress.

Introduction

Heart failure (HF) represents a major burden on the US health care system, with 870,000 new cases annually and a total cost of $30.7 billion. By 2030, the incidence of HF is expected to affect more than 8 million Americans at a cost of almost $70 billion (1). Maladaptive cardiac remodeling is an important step in the progression of HF and is driven by a constellation of cell- and tissue-level factors including hypertrophic growth, inflammation, fibrosis, and genetic reprogramming (2). Growing evidence supports Ca^{2+}/calmodulin-dependent protein kinase II (CaMKII) as a master controller of the maladaptive cardiac remodeling process in failing hearts. Namely, it is well accepted that pathological conditions (e.g., excess Ca^{2+}, β-adrenergic stimulation, oxidative stress) promote the constitutive activation of CaMKII, which in turn leads to dysregulation of a host of intracellular proteins important for cardiac cell excitability, contractility, metabolism, and transcription (3). Recent studies show that genetic deletion of cardiac CaMKII isoforms abrogates systolic dysfunction in response to chronic pressure overload due, in part, to direct effects on gene transcription pathways (4–6). Furthermore, it has become clear that CaMKII is an important node in a larger network of stress-induced kinases and phosphatases linked to pressure overload–induced changes in gene transcription and hypertrophy and HF (2). While great strides have been made in identifying the components of these integrated signaling networks, the field lacks a larger understanding of how the cell tunes the response of an extensive but highly pleiotropic signaling web to a specific perturbation in the cardiac neurohumoral state and/or biomechanical load. At the same time, there has been growing appreciation in the field for the importance of well-defined local signaling domains to maintain spatial and temporal control over pleiotropic networks involved in hypertrophy and HF (7).

Spectrins are important for membrane integrity and ultrastructure (8). Recent studies have demonstrated novel roles for β_{IV}-spectrin in regulating heart function through the organization of local signaling domains (9–11). Specifically, β_{IV}-spectrin targets CaMKII to membrane substrates at the intercalated disc, a specialized cardiac "synapse-like" structure important for intercellular mechanical and electrical communication. Importantly, our group and others have identified significant alterations in spectrins and spectrin-based pathways in human HF and animal models of HF, although the functional consequences are unknown and untested (9–16). On the basis of previous work showing an important role for CaMKII in modulating hypertrophy and HF in response to chronic stress (4–6, 12, 17), we hypothesized that β_{IV}-spectrin may serve as a novel therapeutic target for abrogating adverse cardiac remodeling and HF.

▶ Related Commentary: p. 5219

Conflict of interest: The authors have declared that no conflict of interest exists.

Submitted: December 13, 2017; **Accepted:** September 13, 2018.
Reference information: *J Clin Invest*. 2018;128(12):5561–5572.
https://doi.org/10.1172/JCI99245.

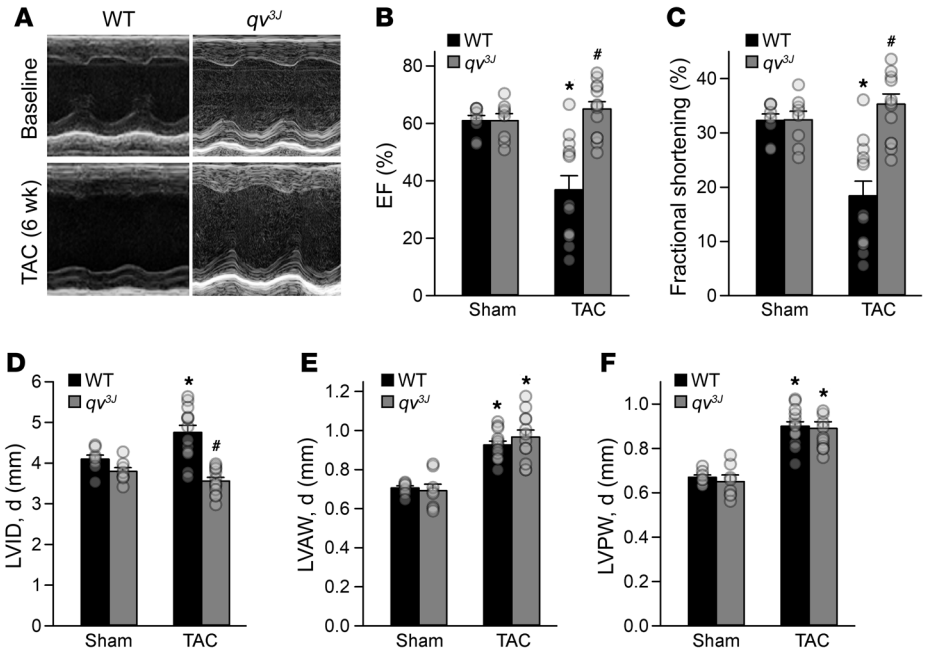

Figure 1. The *qv*^{3J} allele prevents pressure overload–induced pathological remodeling. (**A**) Representative echocardiograms from WT and *qv*^{3J} animals at baseline and following 6 weeks of TAC. (**B**–**F**) Summary data (mean ± SEM) for the echocardiographic features in WT and *qv*^{3J} animals 6 weeks after TAC or sham surgery. $^{*}P < 0.05$ versus sham; $^{\#}P < 0.05$ versus WT, by 2-tailed *t* test. $n = 8$ for WT and *qv*^{3J} sham echocardiographic parameters; $n = 13$ for WT and *qv*^{3J} TAC echocardiographic parameters. LVID, d, LV internal dimension at end diastole; LVAW, d, LV anterior wall thickness at end diastole; LVPW, d, LV posterior wall thickness at end diastole.

Here, we tested the role of the β_{IV}-spectrin–CaMKII complex in modifying the cardiac response to chronic pressure overload. We found that chronic stress promotes CaMKII-dependent degradation of β_{IV}-spectrin and that targeted disruption of spectrin-CaMKII interaction confers protection from pressure overload–induced maladaptive remodeling and cardiac dysfunction without blocking hypertrophy. Unexpectedly, we identified a role for the β_{IV}-spectrin–CaMKII complex in controlling the subcellular localization of STAT3, a ubiquitous stress-activated transcription factor that regulates gene programs important for hypertrophy, fibrosis, and inflammation (18–20). STAT3 signaling is characterized by a high degree of pleiotropy, in which a single transcription factor has been linked to a wide variety of input stimuli and downstream regulatory events. Yet the mechanism underlying the pleiotropic actions of STAT3 remain unclear. Here, we define a direct interaction between β_{IV}-spectrin and STAT3 that is essential for balanced STAT3 signaling and that may imbue the pathway with a degree of pleiotropy. Membrane-bound β_{IV}-spectrin physically sequesters basal STAT3 nuclear transcriptional activity (analogous to cadherin sequestration of β-catenin in the Wnt signaling pathway [ref. 21]). Our data support the idea that dysfunction of the β_{IV}-spectrin–CaMKII complex in disease alters STAT3 sequestration to favor profibrotic pathways and adverse remodeling. These data provide a potential link between spectrin dysfunction and remodeling in HF and establish a paradigm for cardiac β_{IV}-spectrin as a critical regulatory node in a transcriptional highway for stress-induced cellular reprogramming in heart.

Results

Targeted disruption of β_{IV}-spectrin–CaMKII interaction abrogates maladaptive remodeling. Previous work has identified a critical role for CaMKII in controlling the maladaptive response to chronic pressure overload (4–6, 17). Recent studies indicate that β_{IV}-spectrin–associated CaMKII is an important mediator of CaMKII-induced pathological remodeling, although the exact mechanism is undefined (12, 14). Given these findings, we hypothesized that selective targeting of β_{IV}-spectrin–CaMKII interaction would confer protection from pressure overload–induced pathological remodeling. To test this hypothesis, we performed transaortic constriction (TAC) on *qv*^{3J} animals (carrying the spontaneous *qv*^{3J} mutation in *Spnb4*) lacking spectrin-CaMKII interaction and on their WT littermates. The WT animals showed hypertrophy (increased myocyte area and left ventricular [LV] wall thickness) with HF symptoms, including LV dilation and decreased cardiac function following 6 weeks of TAC (Figure 1, A–D and Supplemental Figure 1; supplemental material available online with this article; doi: 10.1172/JCI99245DS1). While *qv*^{3J} animals demonstrated a robust hypertrophic response with TAC similar to that seen in the WT animals (Figure 1, E and F), they maintained normal cardiac function with no evidence of LV dilation. In fact, the ejection fraction (EF) was no different in *qv*^{3J} animals after 6 weeks of TAC compared with baseline EF values (Figure 1B). The *qv*^{3J} animals showed an increased EF and less LV dilation, even up to 10 weeks after TAC compared with WT animals (Supplemental Figure 2). Mortality was low in both groups and not statistically different (12 of 13 WT animals survived out to 10 weeks compared with 8 of 9 *qv*^{3J} animals; P = NS). To evaluate the possibility of systemic alterations in the *qv*^{3J} animals contributing to their differential response to TAC, we measured the metabolic state and body composition in *qv*^{3J} animals and their WT littermates at baseline. We found no baseline metabolic differences that could explain the observed phenotypic difference between WT and *qv*^{3J} animals (Supplemental Figure 3 and Supplemental Table 1).

The β_{IV}-spectrin–CaMKII complex mediates STAT3 dysregulation following TAC. Given the dramatically altered remodeling response to TAC observed in *qv*^{3J} animals, we sought to use an unbiased approach to identify signaling pathways differentially regulated in *qv*^{3J} TAC hearts, potentially downstream of aberrant spectrin-associated CaMKII. We performed microarray and pathway analysis on *qv*^{3J} TAC and WT TAC hearts. Of the 201 genes

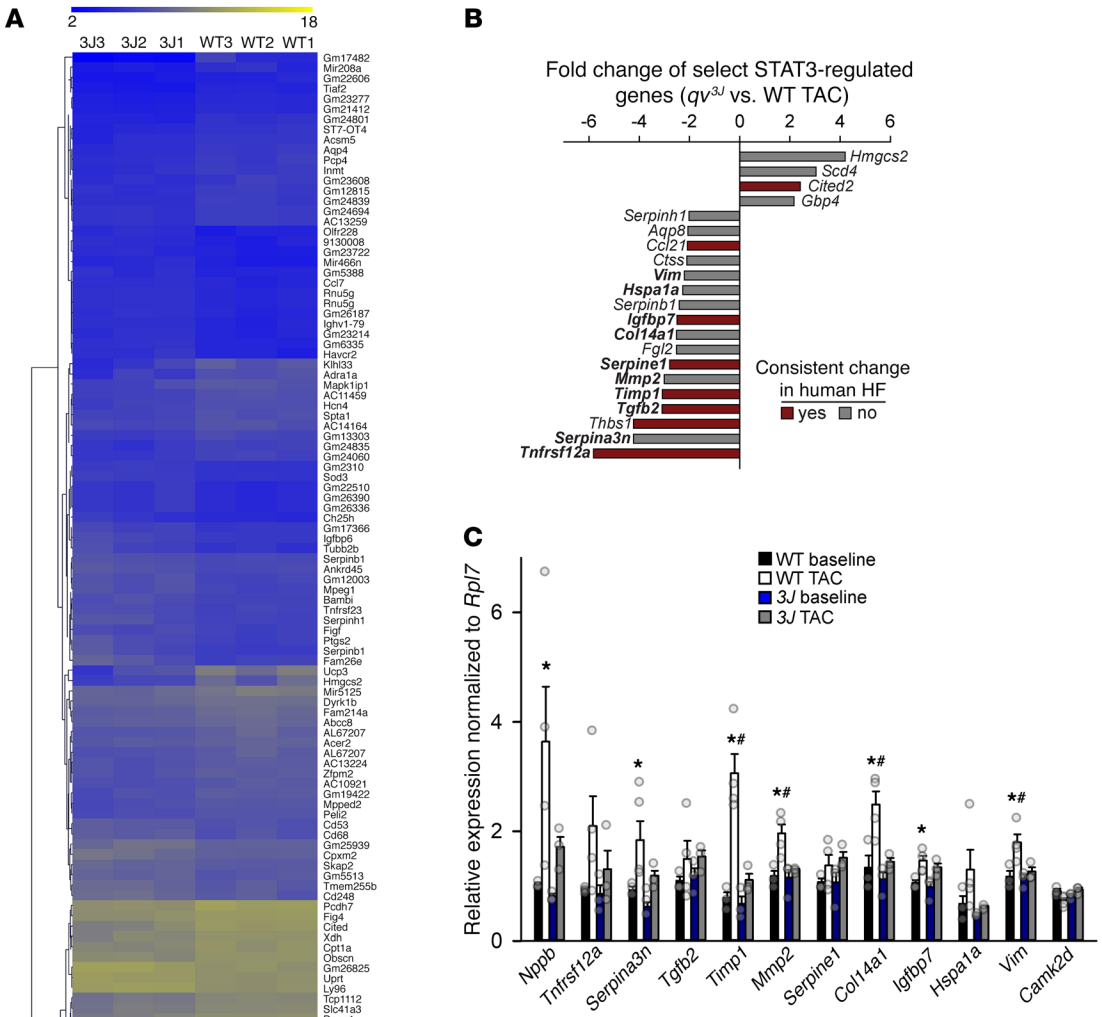

Figure 2. Differential regulation of STAT3-related genes in WT and *qv*^{3J} TAC hearts. (**A**) Heatmap showing the expression profiles of select genes (>1.5-fold change, $P < 0.005$) between WT and *qv*^{3J} TAC hearts analyzed by microarray. $n = 3$ from 3 separate hearts in triplicate per group. (**B**) Fold change of select STAT3-related genes differentially regulated in WT and *qv*^{3J} TAC hearts. Genes with a reported change in human HF consistent with the observed change in WT TAC are indicated in red. (**C**) Selected STAT3-dependent genes (*Nppb*, *Tnfrsf12a*, *Serpina3n*, *Tgfb2*, *Timp1*, *Mmp2*, *Serpine1*, *Col14a1*, *Igfbp7*, *Hspa1a*, and *Vim*) differentially regulated in HF were validated by qPCR. *Camk2d* was not identified in the microarray as being different between WT and *qv*^{3J} hearts (*3J*) and was used as a control. *$P < 0.05$ versus baseline, by 1-way ANOVA with the Holm-Sidak post hoc test (#$P < 0.05$ vs. *qv*^{3J} TAC). $n = 3$ from 3 separate hearts in triplicate for WT baseline, *qv*^{3J} baseline, and *qv*^{3J} TAC; $n = 4$ from 4 separate hearts in triplicate for WT TAC. Summary data are expressed as the mean ± SEM.

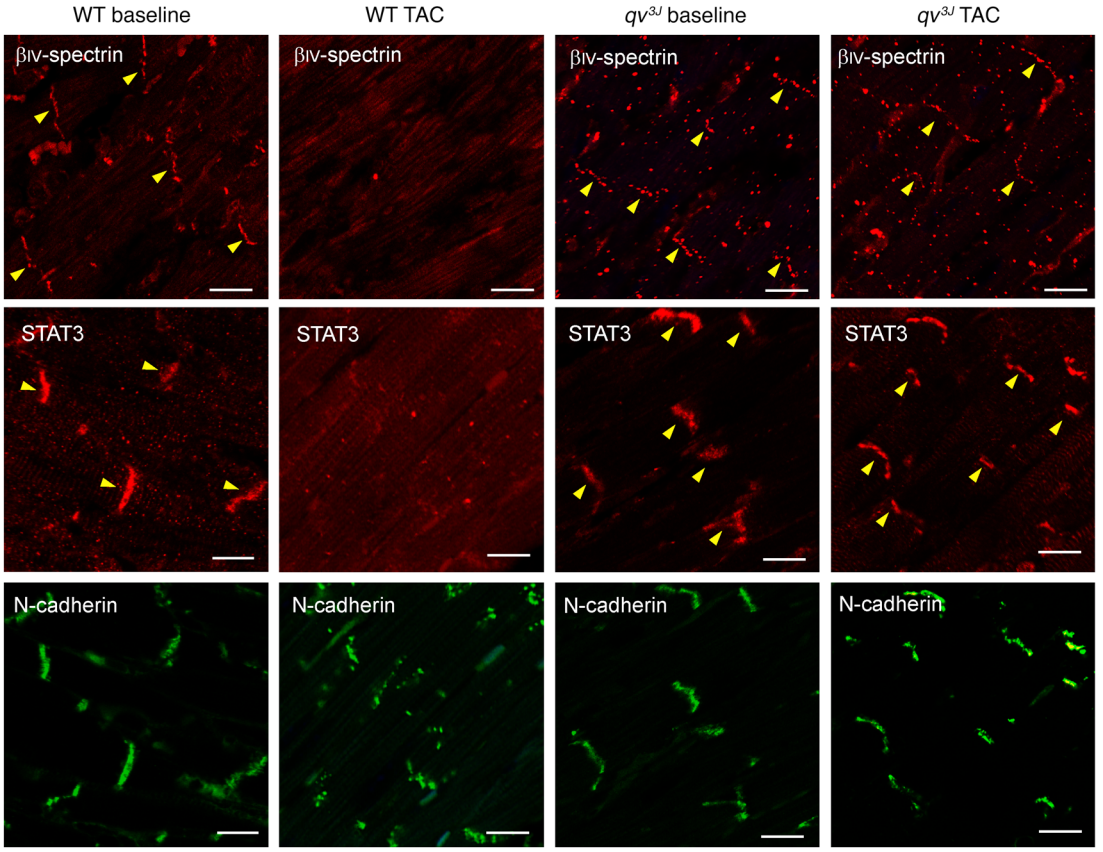

Figure 3. Differential β_{IV}-spectrin expression and STAT3 localization in WT and *qv*^{3J} TAC hearts. Ventricular sections immunostained for β_{IV}-spectrin, STAT3, and N-cadherin. Prominent intercalated disc localization of β_{IV}-spectrin and STAT3 (yellow arrowheads) was apparent in WT baseline, *qv*^{3J} baseline, and *qv*^{3J} TAC hearts, but not WT TAC hearts. Scale bars: 20 μm.

differentially regulated in the 2 groups, 50 had been previously shown to be regulated by the transcription factor STAT3 (Figure 2, A and B, and Supplemental Table 2). Additional analysis using MatInspector bioinformatics software was performed on the 61 genes found to be significantly downregulated in the *qv*^{3J} mouse. A large majority of the targets (47 of 61; Supplemental Table 3) were found to contain a STAT3-binding motif within their promoter region. Moreover, a collective analysis to identify transcription factor motifs abundantly represented throughout these promoter sequences revealed a highly significant association with STAT3 ($P = 5.18 \times 10^{-5}$) but not with other transcription factors previously linked to CaMKII, MEF2, and NFAT (P = NS). Manual curation of STAT3-induced genes showed multiple genes implicated in human HF (Figure 2B). We performed quantitative PCR (qPCR), which confirmed that expression of several STAT3-dependent genes, including *Nppb*, *Serpina3n*, *Timp1*, *Mmp2*, *Col14a1*, and *Vim*, was elevated in WT but not *qv*^{3J} hearts following TAC compared with baseline expression levels (Figure 2C).

Under basal conditions, STAT3 resides in high-molecular-weight complexes, although the molecular constituency of these "statosomes" remains unclear (22). Canonical signaling involves the recruitment of STAT3 to activated JAK at the membrane, leading to phosphorylation at Tyr705, dimerization, and subsequent translocation to the nucleus. Noncanonical pathways involving, for example, the unique effects of unphosphorylated or hyperphosphorylated STAT3, have also been identified (23–25). As a first step in determining whether STAT3 signaling was altered in *qv*^{3J} mice, we analyzed the expression of STAT3 in WT and *qv*^{3J} TAC hearts. Interestingly, under basal conditions, STAT3 was found to be concentrated at the intercalated disc membrane, where our previous studies have shown that β_{IV}-spectrin colocalizes and associates with a subpopulation of CaMKII (Figure 3) (9, 11, 12). Furthermore, loss of β_{IV}-spectrin and STAT3 from the intercalated disc membrane occurred in WT but not *qv*^{3J} hearts following TAC, without any change in total STAT3 levels (Figure 3 and Supplemental Figures 4 and 5). Together, these data indicate that TAC alters the subcellular distribution of STAT3, ostensibly as a result of stress-induced downregulation of β_{IV}-spectrin (10, 26). Furthermore, our data show that targeted ablation of β_{IV}-spectrin–CaMKII interaction in vivo (*qv*^{3J} allele) prevents STAT3 dysregulation and preserves cardiac function in response to chronic pressure overload.

Preservation of β_{IV}-spectrin in *qv*^{3J} TAC hearts led us to ask whether β_{IV}-spectrin was a target for CaMKII itself, with implications for its own stability. As a first step in determining the mechanism underlying stress-induced β_{IV}-spectrin degradation, we subjected isolated WT and *qv*^{3J} ventricular myocytes to long-term stress conditions in vitro (Figure 4, A and B). Following 12 hours of pacing in the presence of isoproterenol and okadaic acid (hyperphosphorylating conditions to increase adrenergic tone), we detected a significant decrease in β_{IV}-spectrin levels in WT but not *qv*^{3J} myo-

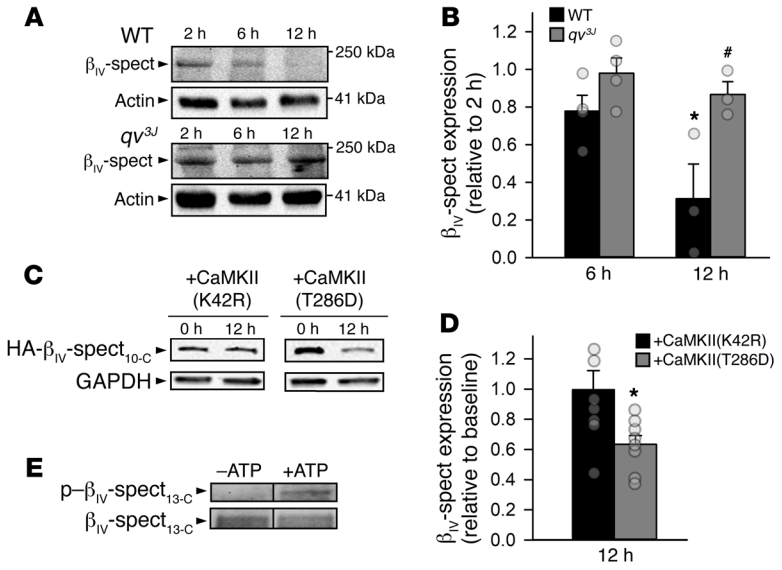

Figure 4. CaMKII promotes the degradation of β_{IV}-spectrin in vitro. (**A** and **B**) Representative immunoblots and densitometric measurements for β_{IV}-spectrin (β_{IV}-spect) (actin was used as a loading control) from isolated WT and *qv*^{3J} myocytes subjected to prolonged pacing (up to 12 hours at 2 Hz) in the presence of isoproterenol and okadaic acid to simulate long-term stress (hyperphosphorylating) conditions. $^{*}P < 0.05$ versus 6 hours; $^{\#}P < 0.05$ versus WT, by 1-way ANOVA with the Holm-Sidak post hoc test. $n = 3$ and 4 from independent preparations for the 6-hour and 12-hour time points, respectively. (**C** and **D**) Representative immunoblots and densitometric measurements from COS-7 cells coexpressing the HA-tagged β_{IV}-spectrin fragment from repeat 10 to the C-terminus (HA-β_{IV}-spect$_{10\text{-}C}$) and either constitutively active [CaMKII(T286D)] or kinase-dead [CaMKII(K42R)] CaMKII. $^{*}P < 0.05$ versus K42R, by 2-tailed *t* test. $n = 8$ per group from independent preparations. (**E**) In vitro phosphorylation assay showing the levels of serine/threonine phosphorylated β_{IV}-spectrin (p–β_{IV}-spect$_{13\text{-}C}$) and total β_{IV}-spectrin (β_{IV}-spect$_{13\text{-}C}$) in the presence of CaMKII, with or without ATP (100 μM).

cytes. Furthermore, loss of β_{IV}-spectrin was prevented in WT myocytes treated with the CaMKII inhibitor KN-93 and in myocytes from AC3-I mice expressing a CaMKII-inhibitory peptide, similar to the protection afforded by the *qv*^{3J} allele (Supplemental Figure 6). In vitro assays demonstrated that overexpression of active CaMKII increased phosphorylation and decreased the expression of β_{IV}-spectrin (Figure 4, C–E), consistent with the hypothesis that local CaMKII activity regulates the stability of β_{IV}-spectrin in response to long-term stress and provides a potential mechanism for resistance to maladaptive remodeling in *qv*^{3J} hearts subjected to TAC.

Given our observation that STAT3 localizes to the myocyte intercalated disc membrane and that dysregulation of STAT3 localization and downstream signaling occur together with loss of β_{IV}-spectrin following TAC, we hypothesized that β_{IV}-spectrin defines a novel signaling complex with STAT3 ("statosome") (ref. 22) to control gene transcription in response to chronic stress. A scan of the full-length β_{IV}-spectrin sequence identified a proline-rich region in spectrin repeat 15, homologous to an identified STAT3-binding sequence in human IL-2γ (27) (Figure 5A and Supplemental Figure 7). We first tested for β_{IV}-spectrin–STAT3 interaction using radiolabeled STAT3 and immobilized β_{IV}-spectrin fragments with or without repeat 15 containing the putative STAT3-binding site. Consistent with a specific interaction, we found that STAT3 bound only to β_{IV}-spectrin fragments containing repeat 15 ($\beta_{IV,10\text{-}17}$, $\beta_{IV,13\text{-}C}$) (Figure 5, B and C). In agreement with in vitro direct binding experiments, $\beta_{IV,13\text{-}C}$ associated with endogenous STAT3 from heart lysates (Figure 5D). Furthermore, coimmunoprecipitation experiments showed that endogenous β_{IV}-spectrin associated with endogenous STAT3 in heart lysates from WT mice but not from mice expressing truncated β_{IV}-spectrin lacking the putative STAT3-binding motif (*qv*^{4J} allele with a premature stop codon in spectrin repeat 10; refs. 10, 28 and Figure 5E). Together, these data demonstrate for the first time to our knowledge that β_{IV}-spectrin interacts directly with STAT3, possibly to coordinate downstream gene expression and a functional response to chronic stress in vivo.

STAT3 dysregulation and cardiac dysfunction in cardiac-specific β_{IV}-spectrin–KO mice. To test the hypothesis that stress-induced loss of β_{IV}-spectrin promotes STAT3 dysregulation, genetic reprogramming, and pathological remodeling, we generated a cardiac-specific β_{IV}-spectrin–KO mouse (αMHC-CRE/*Spnb4*$^{fl/fl}$, referred to hereafter as β_{IV}-cKO) (Figure 6, A and B). Use of a conditional KO allowed us to not only circumvent defects associated with global β_{IV}-spectrin deficiency (28), but also to address the role of β_{IV}-spectrin and STAT3 in myocytes versus other heart cells (fibroblasts, immune cells). β_{IV}-Spectrin was not detectable by immunoblotting or immunostaining in β_{IV}-cKO cardiomyocytes (Figure 6, C and D; Figure 7, A and B; and Supplemental Figure 8), similar to what was observed in WT TAC cardiomyocytes (Figure 3 and Figure 7C). We verified that β_{IV}-spectrin levels were normal in pancreas, which also expresses the isoform (Supplemental Figure 8). We found that expression of other spectrins (β_{II}-spectrin, α_{II}-spectrin) was not affected in β_{IV}-cKO hearts (Supplemental Figure 8). Expression and localization of $Na_v1.5$ were also normal in β_{IV}-cKO compared with WT hearts (Figure 6D and Figure 7, A and B), consistent with previous results indicating β_{IV}-spectrin–independent (but ankyrin-G–dependent) expression of $Na_v1.5$ in heart (10, 11). CaMKII showed a small but significant decrease in β_{IV}-cKO hearts (Figure 6, C and D). Interestingly, while STAT3 levels were normal, its localization was dramatically altered in β_{IV}-cKO myocytes at baseline. Specifically, while STAT3 was highly localized to the intercalated disc in cells and tissue from WT baseline, *qv*^{3J} baseline, and *qv*^{3J} TAC hearts, cardiac-specific deletion of β_{IV}-spectrin resulted in a loss of submembrane STAT3 comparable to that seen in WT TAC hearts (Figure 7, A, B, and D–F). qPCR demonstrated altered expression of STAT3-regulated genes in β_{IV}-cKO hearts, which was consistent with our measurements in WT TAC hearts (Supplemental Figure 9). Together, these data support our hypothesis that β_{IV}-spectrin organizes a "statosome" in heart and that loss of β_{IV}-spectrin in TAC promotes dysregulation of STAT3 signaling.

On the basis of these data, we hypothesized that STAT3 dysregulation at baseline in β_{IV}-cKO animals would lead to pathological remodeling and/or depressed cardiac function at baseline in the absence of stress, similar to what is observed WT TAC hearts. Consistent with our hypothesis, echocardiography revealed a decrease in cardiac function, with a small but significant degree

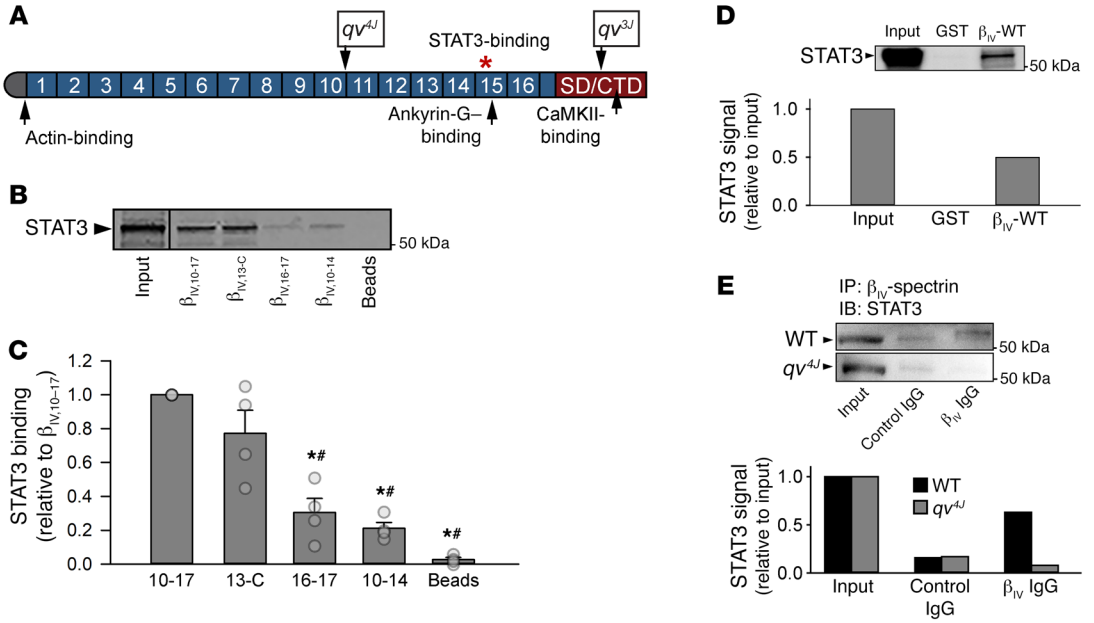

Figure 5. β_{IV}-Spectrin associates with STAT3 in heart. (**A**) β_{IV}-Spectrin is composed of an N-terminal actin-binding domain, 17 spectrin repeats, and C-terminal and specific domains (SD/CTDs). Spectrin repeat 15 contains a putative proline-rich STAT3-binding domain (indicated by a red asterisk). The *qv*^{3J} allele has a targeted defect in spectrin-CaMKII interaction, while the *qv*^{4J} allele also lacks the putative spectrin-STAT3–binding motif. (**B** and **C**) Radiolabeled STAT3 bound immobilized β_{IV}-spectrin fragments that contained repeat 15 (locus of the putative STAT3-binding domain). *$P < 0.05$ versus $\beta_{IV,10-17}$; #$P < 0.05$ versus $\beta_{IV,13-C}$, by 1-way ANOVA with the Holm-Sidak post hoc test. $n = 4$ independent experiments. (**D**) Immunoblot and associated densitometric measurements showing that immobilized β_{IV}-spectrin (repeat 13 through C-terminus, β_{IV}-WT) associated with STAT3 from mouse heart. (**E**) Coimmunoprecipitation studies and associated densitometric measurements demonstrating the association of STAT3 with STAT3 in WT, but not *qv*^{4J}, mice expressing truncated β_{IV}-spectrin lacking repeat 11 through the C-terminus.

of LV dilation at baseline compared with WT cardiac function (Figure 8, A–D). In vivo telemetry recordings revealed a normal electrocardiogram with no arrhythmias at baseline in β_{IV}-cKO animals, but a trend toward increased susceptibility to arrhythmic events with acute stress (exercise plus epinephrine; Supplemental Figure 10). While the functional significance of the small amount of LV dilation in β_{IV}-cKO hearts was unclear, we also found increased fibrosis in β_{IV}-cKO hearts, which may further compromise function compared with WT hearts (Figure 8, E and F). In fact, the degree of fibrosis in β_{IV}-cKO hearts was comparable to levels measured in WT hearts following 6 weeks of TAC. Interestingly, fibrosis in *qv*^{3J} TAC hearts was similar to that seen in WT hearts at baseline, consistent with preserved STAT3 localization and activity and cardiac function in the *qv*^{3J} TAC animals.

Therapeutic benefit of STAT3 inhibition in the setting of β_{IV}-spectrin deficiency. STAT3 signaling has been implicated in the inflammatory and fibrotic response to chronic stress (29–31). Furthermore, as discussed above, β_{IV}-cKO hearts showed abnormal STAT3 localization and increased fibrosis compared with WT hearts at baseline (Figure 8, E and F). To determine the specific

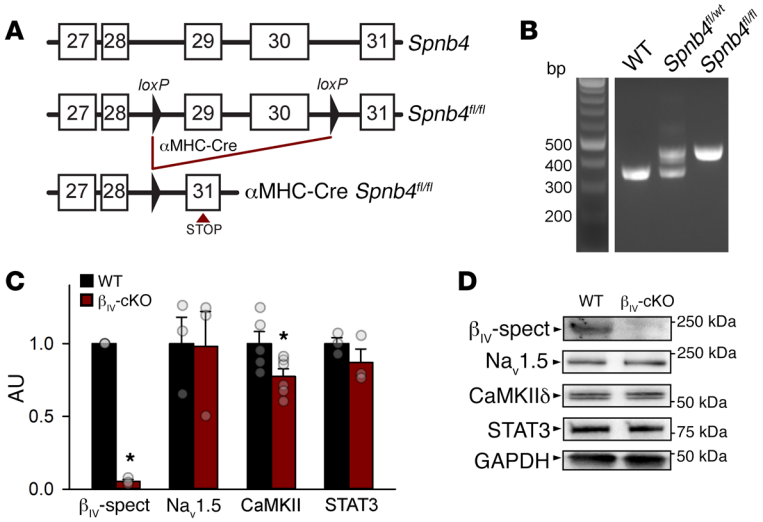

Figure 6. Generation of the cardiac-specific β_{IV}-spectrin–KO mouse. (**A**) Schematic for the generation of the cardiac-specific β_{IV}-cKO mouse. *loxP* sites were inserted into the β_{IV}-spectrin gene (*Spnb4*) flanking exons 29 and 30. Mice homozygous for *loxP* insertion (*Spnb4*$^{fl/fl}$) were crossed with mice expressing Cre recombinase under control of the αMHC promoter to generate experimental mice (αMHC-Cre *Spnb4*$^{fl/fl}$). (**B**) Identification of WT and floxed alleles (341 and 440 bp, respectively) by PCR. (**C** and **D**) Summary data (mean ± SEM) and representative immunoblots of β_{IV}-spectrin, $Na_v1.5$, CaMKII, and STAT3 in WT and β_{IV}-cKO detergent-soluble lysates from myocytes/tissue. *$P <$ 0.05 versus WT by 2-tailed Student's *t* test. $n = 3$ from 3 separate hearts for β_{IV}-spectrin, $Na_v1.5$ and CaMKII for WT and β_{IV}-cKO; $n = 6$ from 6 separate hearts for CaMKII for WT and β_{IV}-cKO.

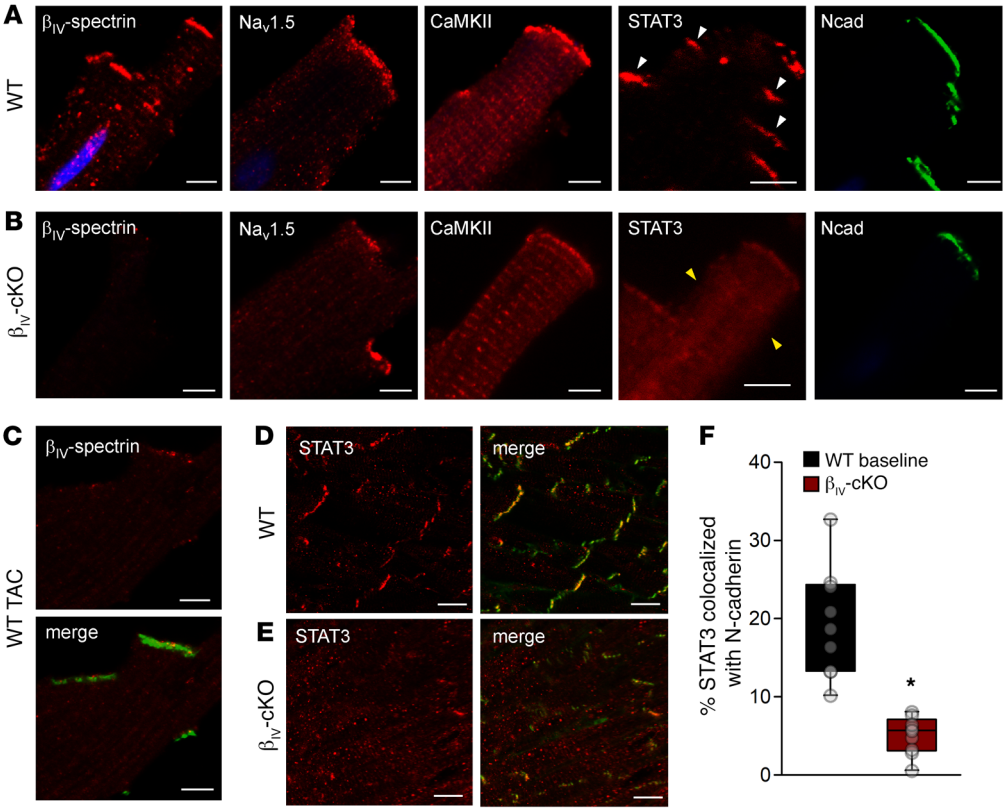

Figure 7. Altered subcellular localization of STAT3 in β_{IV}-specific–deficient myocytes. (**A** and **B**) Permeabilized adult WT and β_{IV}-cKO ventricular myocytes immunostained for β_{IV}-spectrin, $Na_v1.5$, CaMKII, STAT3, and N-cadherin (Ncad). Scale bars: 5 μm. (**C**) Permeabilized adult WT TAC cardiomyocytes immunostained for β_{IV}-spectrin (red) and N-cadherin (green, shown in the merge image). Scale bars: 5 μm. (**D** and **E**) Ventricular sections from WT and β_{IV}-cKO hearts immunostained for STAT3 (red) and N-cadherin (green). Scale bars: 20 μm. (**F**) Summary data (median with 25th and 75th percentiles [box] and 10th and 90th percentiles [whiskers]) showing the percentage of immunoreactive STAT3 signal colocalized with N-cadherin at the intercalated disc. $^*P < 0.05$ versus WT baseline by Mann-Whitney *U* rank-sum test. $n = 9$ cells from 1 heart for WT and β_{IV}-cKO.

role of STAT3 dysregulation in cardiac dysfunction in the setting of β_{IV}-spectrin deficiency, we treated β_{IV}-cKO and WT animals with the selective STAT3 inhibitor S3I-201 (32) (20 mg/kg i.p. daily). STAT3 inhibition significantly improved basal cardiac function at 1 and 2 weeks in β_{IV}-cKO but not WT animals (Figure 9A). In fact, β_{IV}-cKO animals showed a greater than 25% increase in EF with just 1 week of S3I-201 treatment, while WT animals showed no response to the drug. At the same time, STAT3 inhibition eliminated the differences in fibrosis observed in WT and β_{IV}-cKO animals at baseline (compare Figure 9, B and C, with Figure 8, E and F). These data indicate that loss of β_{IV}-spectrin in myocytes contributes to remodeling via a STAT3-dependent pathway. Furthermore, these studies indicate that dysfunction associated with β_{IV}-spectrin deficiency may be ameliorated with STAT3 inhibition.

To test the hypothesis that β_{IV}-spectrin/STAT3 dysfunction promotes remodeling in pressure overload conditions and to determine the therapeutic potential of STAT3 inhibition, we treated WT TAC animals with S3I-201 (20 mg/kg i.p. daily beginning 2 days after surgery until study termination) (Figure 9D). Six weeks after the TAC procedure, the S3I-201–treated animals showed significant improvement in EF compared with baseline, while the untreated animals experienced a greater than 20% decline in function. At the same time, we found that the LV chamber dilation observed in the untreated TAC animals was reversed with S3I-201 treatment. Consistent with our observation in *qv*^{3J} TAC hearts, the drug did not have a significant effect on the hypertrophic ability of the heart (measured by LV anterior wall thickness), although it trended lower in the treated versus untreated hearts. In parallel with the preservation of cardiac function, STAT3 inhibition with S3I-201 abrogated the degree of fibrosis in WT TAC hearts (Figure 8E).

Finally, as an initial effort to determine the relevance of our findings to humans, we assessed nonfailing and failing human heart samples for expression of the STAT3-regulated genes *NPPB*, *TNFRSF12A*, and *COL14A1*, which were confirmed by qPCR to be differentially regulated in WT and *qv*^{3J} TAC hearts and in β_{IV}-cKO hearts. Consistent with our findings in WT TAC and β_{IV}-cKO hearts, we detected an increase in mRNA levels for *NPPB*, *TNFRSF12A*, and *COL14A1*, but not *CAMK2D*, in failing human hearts compared with levels in nonfailing human hearts (Supplemental Figure 11). These findings, together with our previous reports of decreased β_{IV}-spectrin levels in failing human hearts, indicate that the spectrin/STAT3 pathway investigated here may have implications for human disease (10).

Discussion

Despite decades of work, the field lacks a robust model with which to adequately explain the complex cardiac response to chronic pathophysiological stress. Important gaps remain in our under-

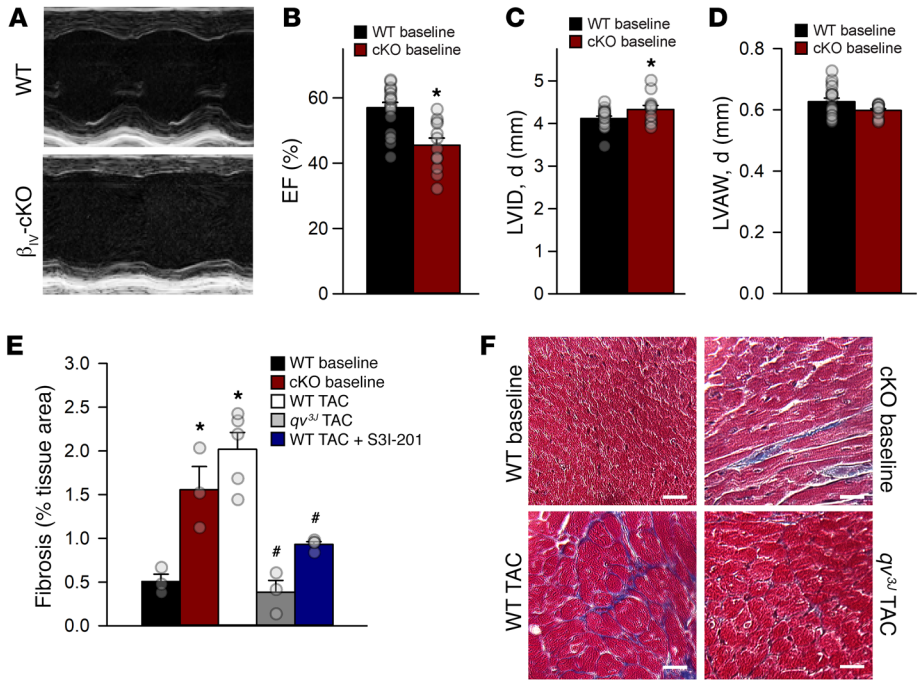

Figure 8. Cardiac-restricted deletion of β_{IV}-spectrin induces maladaptive remodeling at baseline. (**A**) Representative echocardiograms and (**B**–**D**) summary data (mean ± SEM) from WT and cardiac-specific β_{IV}-cKO animals at baseline. $^*P < 0.05$ versus WT, by 2-tailed *t* test. $n = 18$ for WT; $n = 12$ for β_{IV}-cKO. (**E** and **F**) Masson's trichrome–stained heart sections (collagen is labeled in blue) and summary data (mean ± SEM) showing fibrosis as a percentage of the tissue area. $^*P < 0.05$ versus WT baseline; $^{\#}P < 0.05$ versus WT TAC, by 1-way ANOVA with Holm-Sidak post hoc test. $n = 3$ for WT baseline, β_{IV}-cKO baseline, and qv^{3J} TAC; $n = 5$ for WT TAC; $n = 4$ for WT TAC plus the STAT3 inhibitor S3I-201 (20 mg/kg i.p. daily). Scale bars: 200 μm.

standing of the process by which biomechanical and neurohumoral stress induces a specific form of cardiac hypertrophy, and how and why the hypertrophic response may transition to a maladaptive stage characterized by adverse remodeling (fibrosis, ventricular chamber dilation, ventricular wall thinning) and ultimately HF. The conventional view of hypertrophy is that, at least in the short term, it serves an adaptive role, allowing the heart to normalize changes in wall stress induced by increased afterload (33). However, it has been almost 20 years since the seminal observation that LV mass serves as a prognostic indicator for cardiovascular event risk (34). These data and subsequent studies (35–38) have called into question the adaptive nature of hypertrophy, suggesting that perhaps an optimal therapy involves suppressing the hypertrophic response altogether (39). While hypertrophy remains a viable therapeutic target for HF (especially in the presence of preserved EF) (38, 40, 41), our studies using both genetic and pharmacological approaches add to mounting evidence (6, 42) that it is possible to prevent (or at least delay) the transition from an adaptive hypertrophic response to maladaptive remodeling and HF. At the same time, we identify a new β_{IV}-spectrin–based pathway that specifically regulates maladaptive remodeling, making it an attractive potential target for HF therapy. Specifically, we propose that chronic pressure overload induces the disintegration of a key spectrin-based "statosome" that promotes noncanonical and maladaptive STAT3 signaling (Figure 10).

An important unresolved issue to address relates to the complex web of pleiotropic signaling networks linked to hypertrophy and HF (2). CaMKII regulates multiple transcriptional pathways involved in hypertrophy and maladaptive remodeling (e.g., HDAC/MEF2, calcineurin/NFAT) (4, 6, 43). Our data identify β_{IV}-spectrin/STAT3 as a CaMKII-dependent network that specifically regulates the maladaptive response. The question remains: how does the cell decide which networks are activated or suppressed and when in the time course of the cardiac response? Furthermore, how is signaling via distinct but related pathways integrated to determine the phenotype at the cell and organ levels? Clearly, an important determinant is the specific biomechanical/neurohumoral challenge. For example, elegant experiments by the Rockman group showed that the duration of the stimulus has less to do with the specific cardiac response than the nature of the stimulus itself (e.g., physiological vs. pathological challenge) (44). An aspect of our study relevant to this discussion is the focus on local control of a subpopulation of CaMKII/STAT3 at the cardiomyocyte intercalated disc membrane. Interestingly, our findings in the qv^{3J} mouse align with those of recent work showing hypertrophy with preserved systolic function in response to pressure overload in both CaMKII δ-KO and CaMKII δ/γ double-KO mice (5, 6). Although the qv^{3J} allele directly affects only a subpopulation of CaMKII (9), the afforded protection is comparable to complete KO of the 2 cardiac CaMKII isoforms. We propose that this spectrin-based signaling node has evolved for the specific purpose of sensing local, abnormal stress and that β_{IV}-spectrin itself serves as an important target for pathological CaMKII signaling, although potential contributions from other targets (including $Na_v1.5$, Ca^{2+} cycling proteins, and mitochondrial proteins) cannot be ruled out (3, 9, 45, 46). Together, these data suggest that the β_{IV}-spectrin C-terminal domain (CTD) serves as a "pathological" membrane dock for intracellular CaMKII (probably multiple isoforms) and that disruption of this CaMKII subpopulation is sufficient to abrogate maladaptive remodeling in response to chronic stress. While our initial data support a model whereby CaMKII-dependent phosphorylation of β_{IV}-spectrin ultimately leads to its degradation, release of STAT3, and large-scale changes in gene transcription (Figure 10), future studies are required to determine the precise mechanism by which spectrin-associated CaMKII destabilizes spectrin-STAT3 interaction and/or alters STAT3 activity.

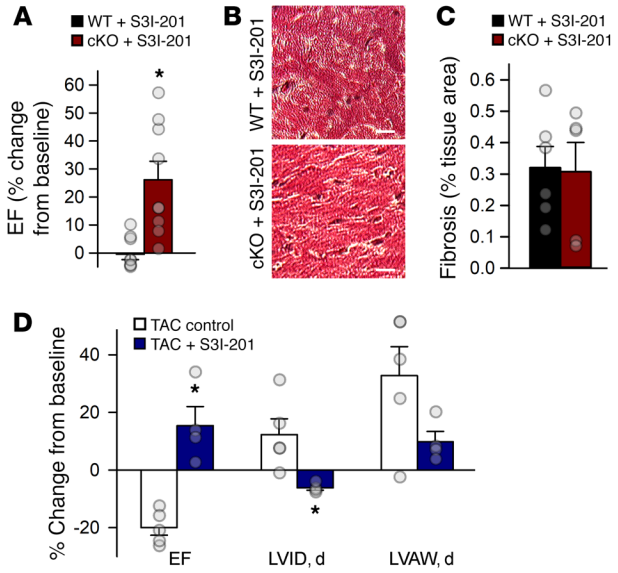

Figure 9. STAT3 inhibition abrogates maladaptive remodeling in cardiac-specific β_{IV}-spectrin–KO mice and with chronic pressure overload. (**A**) Summary data (mean ± SEM) for echocardiographic features in WT and β_{IV}-spectrin–KO (cKO) animals following treatment with the STAT3 inhibitor S3I-201 (20 mg/kg i.p. daily for 1 week). *$P < 0.05$ versus WT, by 2-tailed t test. $n = 9$ for WT and cKO. (**B** and **C**) Masson's trichrome–stained heart sections (collagen is labeled in blue) and summary data (mean ± SEM) showing fibrosis as a percentage of the tissue area. P = NS. $n = 6$ for WT and $n = 5$ for cKO. Scale bars: 100 μm. (**D**) Summary data (mean ± SEM) for echocardiographic features following 6 weeks of TAC, with or without the STAT3 inhibitor S3I-201 (20 mg/kg i.p. daily). *$P < 0.05$ versus TAC control, by 2-tailed t test. $n = 5$ for TAC control and $n = 4$ for TAC plus S3I-201.

While our findings show that disruption of β_{IV}-spectrin–CaMKII interaction in vivo preserves the integrity of the β_{IV}-spectrin–STAT3 complex and prevents maladaptive remodeling in response to chronic pressure overload, we cannot rule out the possibility of a contribution to the phenotype of STAT3-independent pathways. CaMKII targets a large number of intracellular substrates (ion channels, Ca^{2+} cycling proteins, transcription factors other than STAT3, mediators of inflammatory response) that are potentially important in regulating the hypertrophic/HF response (3, 47, 48). It is likely that direct or indirect changes in activity of several of these targets play a role in the protection afforded by the qv^{3J} allele. At the same time, it is likely that cardiac cells (e.g., fibroblasts and immune cells) other than myocytes are affected in the qv^{3J} mouse (global truncation of β_{IV}-spectrin) and may mediate the altered remodeling response with TAC. Likewise, we cannot rule out the possibility of a role for other signaling pathways independent of CaMKII. In this regard, a fascinating avenue for further study is related to signaling between the lipid bilayer and spectrin. Despite these limitations, our data support a central role for the spectrin-based cytoskeleton in the heart's adaptation to chronic stress and identify targets to modify this response for therapeutic benefit.

Discovered as structural proteins in the erythrocyte membrane (8), spectrins are classically viewed as "static" adapter proteins responsible for maintaining membrane integrity. However, our findings in multiple excitable cell types support spectrins as critical signaling nodes (9, 16). Our new data expand the roles of spectrins (in any cell) as tunable sensors of the cellular stress response, serving to modulate key transcriptional pathways important for fibrotic response and cardiac function. Specifically, we propose that β_{IV}-spectrin organizes a critical "statosome" in cardiac myocytes to preserve temporal and spatial control over STAT3 signaling (22) (Figure 10). Although previous work has identified a potential feedback mechanism between β_{II}-spectrin (encoded by *Sptbn1* in the mouse) levels and STAT3 expression (49), we did not find evidence that β_{IV}-spectrin controls the expression of STAT3 itself in cardiomyocytes; rather, we found that it controls STAT3 subcellular localization and activity, perhaps reflecting functional differences across β-spectrin isoforms (e.g., β_{II}-spectrin vs. β_{IV}-spectrin). At the same time, earlier work has uncovered an association between spectrin and TGF-β/SMAD signaling, with potential implications for remodeling responses to pressure overload (50). While we cannot rule out the possibility of a role for TGF-β/SMAD independent of STAT3 in the β_{IV}-spectrin–deficient phenotype, it is interesting to note that STAT3 controls the expression of a wide variety of genes including TGF-β and may serve as the key node linking spectrin to other signaling pathways.

Despite prior work showing dysregulation of STAT3 in animal models and human disease (18, 19, 51–53), the in vivo roles of STAT3 remain unclear and controversial. On one hand, studies using

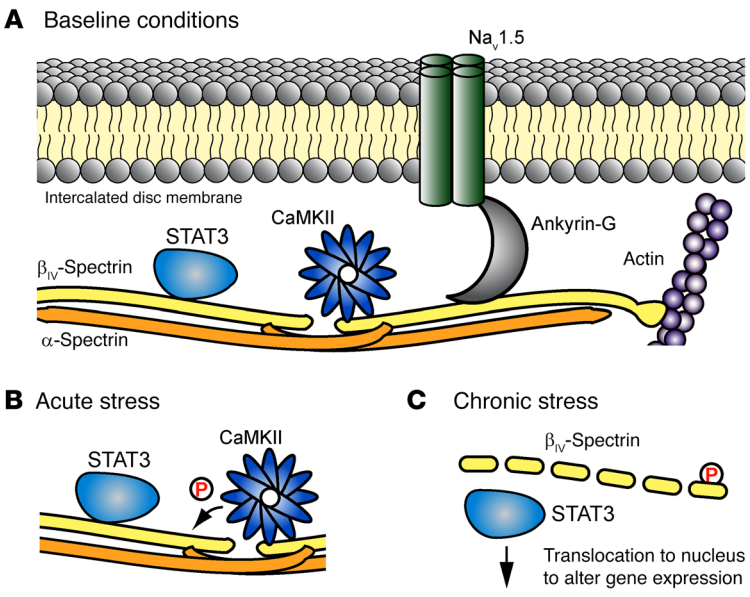

Figure 10. Schematic of proposed spectrin-based complex to regulate gene expression in response to chronic stress. (**A**) Spectrin-based macromolecular complex at the cardiomyocyte intercalated disc membrane, which is composed of β_{IV}-spectrin, CaMKII, and STAT3. Previous studies have identified the association with cardiac voltage–gated Na^+ channel $Na_v1.5$ via the adapter protein ankyrin-G. (**B** and **C**) CaMKII activation during stress leads to phosphorylation of β_{IV}-spectrin and eventual degradation, releasing STAT3 and allowing for its translocation to the nucleus, where it is able to induce profibrotic genes.

genetic mouse models support the notion that STAT3 is protective against acute and chronic stress in heart as a result of antiapoptotic and antioxidant effects (20, 54–56). On the other hand, continuous STAT3 activation is associated with worse outcomes in myocardial infarction, HF, and atrial fibrillation because of proinflammatory, profibrotic pressure (29, 30, 32). Confusion regarding the role of STAT3 stems in part from limitations of animal models and reagents that suffer from (a) a lack of fine control (STAT3 is either completely eliminated or constitutively active), and/or (b) an inability to study "local" versus "global" regulation of STAT3 signaling. We believe our data provide resolution to the apparent conflicting hypotheses regarding STAT3 function in heart, illustrating that, like β-catenin/Wnt signaling (21), tightly balanced regulation of STAT3-localized activity is required for normal heart function, with loss of balance promoting maladaptive cardiac remodeling in chronic disease.

Methods

Animals. *qv*^{3J} and *qv*^{4J} mice were obtained from The Jackson Laboratory (9, 10, 28). WT littermate mice were used as controls. β_{IV}-spectrin conditional KO mice were generated (genOway) on a C57/Bl6 background using an Flp-mediated strategy to remove the neomycin selection cassette. Genotyping was performed by PCR using the following primers: 5′-GAGCTGCATAAGTTCTTCAGCGATGC-3′ (sense) and 5′-ACCCCATCTCAACTGGCTTTCTTGG-3′ (antisense), yielding bands of 341 and 440 bp for WT and floxed alleles, respectively. The resulting animals expressing the floxed spectrin allele were crossed with mice expressing Cre under the cardiac promoter α-myosin heavy chain (αMHC-Cre, purchased from The Jackson Laboratory), resulting in cardiac-specific deletion of β_{IV}-spectrin (αMHC-*Spnb4*$^{fl/fl}$). Experiments were performed in 2-month-old male mice. Animals were euthanized using CO_2 and cervical dislocation followed by collection of tissue or cell isolation.

Murine HF model with proximal aortic banding. TAC was performed to induce pressure overload conditions in adult male mice (12, 16). Mice were anesthetized (isoflurane, 2.5%), intubated, and placed on a respirator (120 breaths per minute – 1; 0.1 ml tidal volume). A midline sternotomy was performed to expose the aorta, and a 7.0 Prolene suture was placed around the aorta distal to the brachiocephalic artery. The suture was tightened using a blunted 27-gauge needle next to the aorta as a guide for the degree of aortic constraint, the needle was removed, and the chest was closed. A group of sex- and age-matched sham mice underwent the same procedure, with the suture step omitted as a control. Echocardiography using the Vevo 2100 (VisualSonics) was performed before surgery and at regular intervals for 6 or 10 weeks following surgery to assess cardiac function. The MS-400 transducer was used in the short-axis M-mode to assess cardiac function. Mice were sacrificed 6 weeks after TAC or sham surgery. Hearts were gathered from each mouse for further analysis.

Adult myocyte pacing experiments. Ventricular myocytes from WT and *qv*^{3J} adult mice were isolated and plated onto a 6-well tray precoated with laminin (Invitrogen, Thermo Fisher Scientific), as described previously (14). Cells were pretreated for 30 minutes with the phosphatase inhibitor okadaic acid (MilliporeSigma, 2 μm) and paced (amplitude = 35 V, duration = 3 ms) for 2 hours, 6 hours, or 12 hours at 2 Hz using the C-pace multichannel stimulator (Ionoptix) with isoproterenol (MilliporeSigma, 100 nM) added to the media just prior to the onset of pacing. A subset of experiments were conducted on myocytes isolated from AC3-I mice (gift of Mark Anderson, Johns Hopkins University School of Medicine, Baltimore, Maryland, USA) with cardiac-specific expression of a CaMKII-inhibitory peptide (14),or on WT cells pretreated for 30 minutes with the CaMKII inhibitor KN-93 (MilliporeSigma, 10 μM) or the inactive analog KN-92 (MilliporeSigma, 10 μM). Cell lysates were analyzed by SDS-PAGE and immunoblotting.

Microarray and qPCR. Total RNA from mouse heart tissues was extracted with TRIzol Reagent plus RNeasy column purification (QIAGEN) following the manufacturer's instructions. RNA integrity was analyzed using the Agilent 2100 Bioanalyzer (Agilent Technologies). A 100-ng aliquot of total RNA was linearly amplified, and 5.5 μg cDNA was labeled and fragmented using the GeneChip WT PLUS Reagent Kit (Affymetrix) according to the manufacturer's instructions. Labeled cDNA targets were hybridized to the Affymetrix GeneChip Mouse Transcriptome Array 1.0 for 16 hours at 45°C. The arrays were washed and stained using the Fluidics Station 450 and scanned using the GeneChip Scanner 3000. For gene expression analysis (>29,000 genes), the arrays were normalized using the RMA-SST algorithm in Expression Console, and comparisons were made with the Transcriptome Analysis Console (Affymetrix). Genes with a *P* value cutoff below 0.05 and a fold change of greater than 1.5 were used for pathway analysis (Ingenuity Pathway Analysis, QIAGEN Inc., www.qiagenbioinformatics.com/products/ingenuity-pathway-analysis/) and for analysis of transcription factor binding using MatInspector (Genomatrix). Select genes (*Nppb*, *Camk2d*, *Tnfrsf12a*, *Serpina3n*, *Tgfb2*, *Timp1*, *Mmp2*, *Serpine1*, *Col14a1*, *Igfbp7*, *Hspa1a*, and *Vim*) were confirmed by quantitative real-time PCR (qPCR) analysis, as described previously (10). The primer sequences for mice and humans are provided in Supplemental Tables 4 and 5. Total RNA (500 ng), treated with DNase I, was used for first-strand complementary DNA synthesis with the SuperScript III Reverse Transcriptase VILO cDNA Synthesis Kit (Invitrogen, Thermo Fisher Scientific). qPCR reactions were performed in triplicate on cDNA samples in 96-well optical plates with TaqMan Gene Expression Assays (Life Technologies, Thermo Fisher Scientific) and TaqMan Universal PCR Master Mix (No AmpErase UNG, Thermo Fisher Scientific) to maximize PCR precision and uniformity. PCR was performed at 95°C for 3 minutes, followed by 40 cycles of 95°C for 15 seconds and 60°C for 1 minute on an Applied Biosystems 7900HT Fast Real-Time PCR System or a StepOnePlus Real-Time PCR System (Life Technologies, Thermo Fisher Scientific). PCR data were analyzed using the relative standard curve method, and the ΔΔCt method was used to calculate fold changes in relative gene expression. PCR products were confirmed by melt-curve analysis, amplicon length, and DNA sequencing. *Rpl7* levels were used as a normalization control.

Human tissue. LV tissue was obtained from explanted hearts from patients undergoing heart transplantation at The Ohio State University. LV tissue from nonfailing donor hearts not suitable for transplantation was obtained through Lifeline of Ohio.

Statistics. SigmaPlot 13.0 (Systat Software) was used for statistical analysis. Data distribution for all comparisons was first tested for normality using the Shapiro-Wilk test. A 2-tailed *t* test or Mann-Whitney *U* rank-sum test was used to determine *P* values for single comparisons, and a *P* value of less than 0.05 was considered significant. Multiple comparisons were performed using either a 1-way ANOVA with the Holm-Sidak post hoc test (data are presented as the mean ± SEM) or 1-way ANOVA on ranks with Dunn's multiple comparisons test for determination of significant *P* values (data are presented as the median with 25th and 75th percentiles [box] and 10th and 90th percentiles [whiskers]). A *P* value of less than 0.05 was considered significant.

Study approval. Animal studies were conducted in accordance with the NIH's *Guide for the Care and Use of Laboratory Animals* (National Academies Press, 2011), following protocols that were reviewed and approved by the IACUC of The Ohio State University. Approval for the use of tissue from human subjects was obtained from the IRB of The Ohio State University. The study conformed with the principles outlined in the Declaration of Helsinki.

See Supplemental Methods for additional details on the methods.

Author contributions

SDU, KIS, SS, PJM, and TJH designed the research studies. SDU, AGS, NP, TH, XX, BO, TS, DH, CL, AD, SNK, DN, ACL, LAB, and HM conducted the experiments. SDU, KIS, and TJH analyzed the data. SDU and TJH wrote the manuscript. SDU, SS, PJM, and TJH edited the manuscript.

Acknowledgments

This work was supported by the NIH (HL114893 and HL135096, to TJH; HL134824, to TJH and PJM; HL114383 and HL135754, to PJM; HL135437 to SAS; HL138738 to KIS; HL129766 to BO; and 5T32HL098039, to AGS); the James S. McDonnell Foundation and the Saving Tiny Hearts Society (to TJH); the American Heart Association (postdoctoral fellowships to SU and AGS); a TriFit Challenge grant from Ross Heart Hospital and Davis Heart and Lung Research Institute; and the OSU Comprehensive Cancer Center Genomics Shared Resource (P30CA016058).

Address correspondence to: Thomas J. Hund, The Dorothy M. Davis Heart and Lung Research Institute, The Ohio State University Wexner Medical Center, 473 W. 12th Avenue, Columbus, Ohio 43210, USA. Phone: 614.292.0755; Email: Thomas.Hund@osumc.edu.

1. Writing Group Members, et al. Heart disease and stroke statistics–2016 update: A report from the American Heart Association. *Circulation*. 2016;133(4):e38–360.
2. Bernardo BC, Weeks KL, Pretorius L, McMullen JR. Molecular distinction between physiological and pathological cardiac hypertrophy: experimental findings and therapeutic strategies. *Pharmacol Ther*. 2010;128(1):191–227.
3. Swaminathan PD, Purohit A, Hund TJ, Anderson ME. Calmodulin-dependent protein kinase II: linking heart failure and arrhythmias. *Circ Res*. 2012;110(12):1661–1677.
4. Backs J, et al. The delta isoform of CaM kinase II is required for pathological cardiac hypertrophy and remodeling after pressure overload. *Proc Natl Acad Sci U S A*. 2009;106(7):2342–2347.
5. Ling H, et al. Requirement for Ca^{2+}/calmodulin-dependent kinase II in the transition from pressure overload-induced cardiac hypertrophy to heart failure in mice. *J Clin Invest*. 2009;119(5):1230–1240.
6. Kreusser MM, et al. Cardiac CaM Kinase II genes δ and γ contribute to adverse remodeling but redundantly inhibit calcineurin-induced myocardial hypertrophy. *Circulation*. 2014;130(15):1262–1273.
7. Lohse MJ, Hofmann KP. Spatial and temporal aspects of signaling by G-protein-coupled receptors. *Mol Pharmacol*. 2015;88(3):572–578.
8. Bennett V, Baines AJ. Spectrin and ankyrin-based pathways: metazoan inventions for integrating cells into tissues. *Physiol Rev*. 2001;81(3):1353–1392.
9. Hund TJ, et al. A β(IV)-spectrin/CaMKII signaling complex is essential for membrane excitability in mice. *J Clin Invest*. 2010;120(10):3508–3519.
10. Hund TJ, et al. β(IV)-Spectrin regulates TREK-1 membrane targeting in the heart. *Cardiovasc Res*. 2014;102(1):166–175.
11. Makara MA, et al. Ankyrin-G coordinates intercalated disc signaling platform to regulate cardiac excitability in vivo. *Circ Res*. 2014;115(11):929–938.
12. Glynn P, et al. Voltage-gated sodium channel phosphorylation at Ser571 regulates late current, arrhythmia, and cardiac function in vivo. *Circulation*. 2015;132(7):567–577.
13. Hund TJ, Wright PJ, Dun W, Snyder JS, Boyden PA, Mohler PJ. Regulation of the ankyrin-B-based targeting pathway following myocardial infarction. *Cardiovasc Res*. 2009;81(4):742–749.
14. Koval OM, et al. Ca^{2+}/calmodulin-dependent protein kinase II-based regulation of voltage-gated Na+ channel in cardiac disease. *Circulation*. 2012;126(17):2084–2094.
15. Smith SA, et al. Dysfunction of the β2-spectrin-based pathway in human heart failure. *Am J Physiol Heart Circ Physiol*. 2016;310(11):H1583–H1591.
16. Smith SA, et al. Dysfunction in the βII spectrin-dependent cytoskeleton underlies human arrhythmia. *Circulation*. 2015;131(8):695–708.
17. Zhang T, et al. The deltaC isoform of CaMKII is activated in cardiac hypertrophy and induces dilated cardiomyopathy and heart failure. *Circ Res*. 2003;92(8):912–919.
18. Haghikia A, Ricke-Hoch M, Stapel B, Gorst I, Hilfiker-Kleiner D. STAT3, a key regulator of cell-to-cell communication in the heart. *Cardiovasc Res*. 2014;102(2):281–289.
19. Zouein FA, Altara R, Chen Q, Lesnefsky EJ, Kurdi M, Booz GW. Pivotal importance of STAT3 in protecting the heart from acute and chronic stress: new advancement and unresolved issues. *Front Cardiovasc Med*. 2015;2:36.
20. Kunisada K, et al. Signal transducer and activator of transcription 3 in the heart transduces not only a hypertrophic signal but a protective signal against doxorubicin-induced cardiomyopathy. *Proc Natl Acad Sci U S A*. 2000;97(1):315–319.
21. Dawson K, Aflaki M, Nattel S. Role of the Wnt-Frizzled system in cardiac pathophysiology: a rapidly developing, poorly understood area with enormous potential. *J Physiol (Lond)*. 2013;591(6):1409–1432.
22. Ndubuisi MI, Guo GG, Fried VA, Etlinger JD, Sehgal PB. Cellular physiology of STAT3: Where's the cytoplasmic monomer? *J Biol Chem*. 1999;274(36):25499–25509.
23. Yue H, Li W, Desnoyer R, Karnik SS. Role of nuclear unphosphorylated STAT3 in angiotensin II type 1 receptor-induced cardiac hypertrophy. *Cardiovasc Res*. 2010;85(1):90–99.
24. Yang J, et al. Novel roles of unphosphorylated STAT3 in oncogenesis and transcriptional regulation. *Cancer Res*. 2005;65(3):939–947.
25. Sehgal PB. Paradigm shifts in the cell biology of STAT signaling. *Semin Cell Dev Biol*. 2008;19(4):329–340.
26. Unudurthi SD, et al. Two-pore K^+ channel TREK-1 regulates sinoatrial node membrane excitability. *J Am Heart Assoc*. 2016;5(4):e002865.
27. Tsujino S, Miyazaki T, Kawahara A, Maeda M, Taniguchi T, Fujii H. Critical role of the membrane-proximal, proline-rich motif of the interleukin-2 receptor gammac chain in the Jak3-independent signal transduction. *Genes Cells*. 1999;4(6):363–373.
28. Parkinson NJ, et al. Mutant beta-spectrin 4 causes auditory and motor neuropathies in quivering mice. *Nat Genet*. 2001;29(1):61–65.
29. Hilfiker-Kleiner D, et al. Continuous glycoprotein-130-mediated signal transducer and activator of transcription-3 activation promotes inflammation, left ventricular rupture, and adverse outcome in subacute myocardial infarction. *Circulation*. 2010;122(2):145–155.
30. Yajima T, et al. Absence of SOCS3 in the cardiomyocyte increases mortality in a gp130-dependent manner accompanied by contractile dysfunction and ventricular arrhythmias. *Circulation*. 2011;124(24):2690–2701.
31. Zhao L, et al. Deletion of interleukin-6 attenuates pressure overload-induced left ventricular hypertrophy and dysfunction. *Circ Res*. 2016;118(12):1918–1929.
32. Huang Z, et al. Signal transducer and activator of transcription 3/microRNA-21 feedback loop contributes to atrial fibrillation by promoting atrial fibrosis in a rat sterile pericarditis model. *Circ Arrhythm Electrophysiol*. 2016;9(7):e003396.
33. Grossman W, Jones D, McLaurin LP. Wall stress and patterns of hypertrophy in the human left ventricle. *J Clin Invest*. 1975;56(1):56–64.
34. Levy D, Garrison RJ, Savage DD, Kannel WB, Castelli WP. Prognostic implications of echocardiographically determined left ventricular mass in the Framingham Heart Study. *N Engl J Med*. 1990;322(22):1561–1566.
35. Sussman MA, et al. Prevention of cardiac hypertrophy in mice by calcineurin inhibition. *Science*. 1998;281(5383):1690–1693.
36. Hill JA, et al. Cardiac hypertrophy is not a required compensatory response to short-term pressure overload. *Circulation*.

2000;101(24):2863–2869.
37. Esposito G, et al. Genetic alterations that inhibit in vivo pressure-overload hypertrophy prevent cardiac dysfunction despite increased wall stress. *Circulation*. 2002;105(1):85–92.
38. Hill JA, et al. Targeted inhibition of calcineurin in pressure-overload cardiac hypertrophy. Preservation of systolic function. *J Biol Chem*. 2002;277(12):10251–10255.
39. Schiattarella GG, Hill JA. Inhibition of hypertrophy is a good therapeutic strategy in ventricular pressure overload. *Circulation*. 2015;131(16):1435–1447.
40. Kong Y, et al. Suppression of class I and II histone deacetylases blunts pressure-overload cardiac hypertrophy. *Circulation*. 2006;113(22):2579–2588.
41. Spiltoir JI, et al. BET acetyl-lysine binding proteins control pathological cardiac hypertrophy. *J Mol Cell Cardiol*. 2013;63:175–179.
42. Crozatier B, Ventura-Clapier R. Inhibition of hypertrophy, per se, may not be a good therapeutic strategy in ventricular pressure overload: other approaches could be more beneficial. *Circulation*. 2015;131(16):1448–1457.
43. Backs J, Song K, Bezprozvannaya S, Chang S, Olson EN. CaM kinase II selectively signals to histone deacetylase 4 during cardiomyocyte hypertrophy. *J Clin Invest*. 2006;116(7):1853–1864.
44. Perrino C, et al. Intermittent pressure overload triggers hypertrophy-independent cardiac dysfunction and vascular rarefaction. *J Clin Invest*. 2006;116(6):1547–1560.
45. Joiner ML, et al. CaMKII determines mitochondrial stress responses in heart. *Nature*. 2012;491(7423):269–273.
46. Ai X, Curran JW, Shannon TR, Bers DM, Pogwizd SM. Ca2+/calmodulin-dependent protein kinase modulates cardiac ryanodine receptor phosphorylation and sarcoplasmic reticulum Ca2+ leak in heart failure. *Circ Res*. 2005;97(12):1314–1322.
47. Weinreuter M, et al. CaM Kinase II mediates maladaptive post-infarct remodeling and pro-inflammatory chemoattractant signaling but not acute myocardial ischemia/reperfusion injury. *EMBO Mol Med*. 2014;6(10):1231–1245.
48. Singh MV, et al. Ca^{2+}/calmodulin-dependent kinase II triggers cell membrane injury by inducing complement factor B gene expression in the mouse heart. *J Clin Invest*. 2009;119(4):986–996.
49. Lin L, et al. Transcriptional regulation of STAT3 by SPTBN1 and SMAD3 in HCC through cAMP-response element-binding proteins ATF3 and CREB2. *Carcinogenesis*. 2014;35(11):2393–2403.
50. Tang Y, Katuri V, Dillner A, Mishra B, Deng CX, Mishra L. Disruption of transforming growth factor-beta signaling in ELF beta-spectrin-deficient mice. *Science*. 2003;299(5606):574–577.
51. Ng DC, Court NW, dos Remedios CG, Bogoyevitch MA. Activation of signal transducer and activator of transcription (STAT) pathways in failing human hearts. *Cardiovasc Res*. 2003;57(2):333–346.
52. Podewski EK, et al. Alterations in Janus kinase (JAK)-signal transducers and activators of transcription (STAT) signaling in patients with end-stage dilated cardiomyopathy. *Circulation*. 2003;107(6):798–802.
53. Uozumi H, et al. gp130 plays a critical role in pressure overload-induced cardiac hypertrophy. *J Biol Chem*. 2001;276(25):23115–23119.
54. Zouein FA, et al. Role of STAT3 in angiotensin II-induced hypertension and cardiac remodeling revealed by mice lacking STAT3 serine 727 phosphorylation. *Hypertens Res*. 2013;36(6):496–503.
55. Enomoto D, Obana M, Miyawaki A, Maeda M, Nakayama H, Fujio Y. Cardiac-specific ablation of the STAT3 gene in the subacute phase of myocardial infarction exacerbated cardiac remodeling. *Am J Physiol Heart Circ Physiol*. 2015;309(3):H471–H480.
56. Zhang W, et al. Critical roles of STAT3 in β-adrenergic functions in the heart. *Circulation*. 2016;133(1):48–61.